

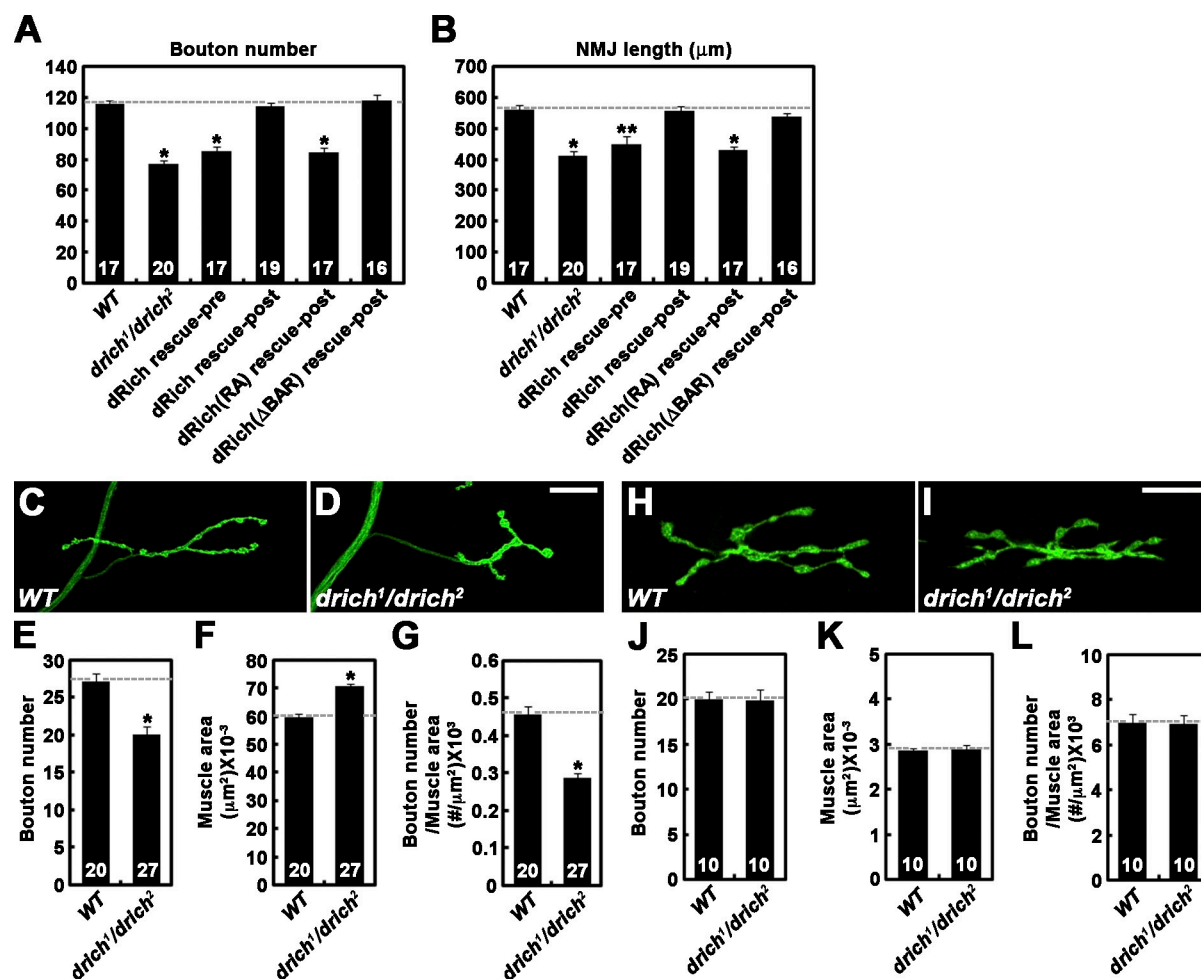
Nahm et al., <http://www.jcb.org/cgi/content/full/jcb.201007086/DC1>

Figure S1. **dRich regulates synaptic growth at the NMJ.** (A and B) *drich* mutations cause synaptic undergrowth at NMJ 6/7. Bouton number (A) and NMJ length (B) at third instar larval NMJ 6/7 were quantified in the following genotypes: wild type (WT), *drich¹/drich²*, *C155-GAL4/+; drich²/UAS-drich, drich¹* (*dRich rescue-pre*), *BG57-GAL4, drich²/UAS-drich, drich¹* (*dRich rescue-post*), *BG57-GAL4, drich²/UAS-drich-R287A, drich¹* (*dRich[RA] rescue-post*), and *BG57-GAL4, drich²/UAS-drichΔBAR-GFP, drich¹* (*dRich[ΔBAR] rescue-post*). (C–G) *drich* mutations cause synaptic undergrowth at NMJ 4. (C and D) Confocal images of NMJ 4 stained with anti-HRP are shown for wild-type (C) and *drich¹/drich²* (D) third instar larvae. Bars, 25 μm. (E–G) Quantification of total bouton number (E), surface area of muscle 4 (F), and bouton number normalized to muscle surface area (G). (H–L) Muscle and NMJ growth are normal in *drich* early first instar larvae. (H and I) Confocal images of NMJs 6/7 stained with anti-HRP are shown for wild-type (H) and *drich¹/drich²* (I) early first instar larvae (within 1 h after hatching). Bar, 10 μm. (J–L) Quantification of total bouton number (J), combined surface area of muscles 6 and 7 (K), and bouton number normalized to muscle surface area (L). Statistically significant differences versus wild type are indicated. *, $P < 0.001$; **, $P < 0.01$. Error bars indicate mean \pm SEM.

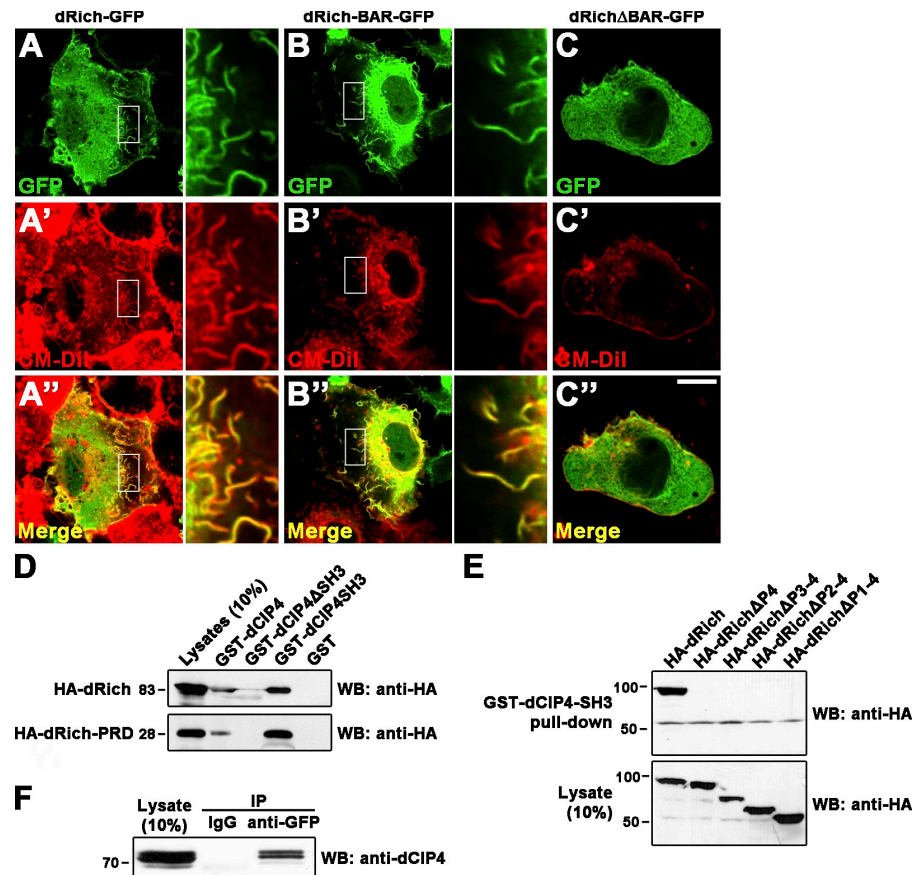


Figure S2. Characterization of BAR and proline-rich domains of dRich. (A–C'') dRich has a functional BAR domain. Mammalian COS-7 cells were transiently transfected with a plasmid encoding dRich-GFP (A), dRich-BAR-GFP (B), or dRichΔBAR-GFP (C) and stained with 10 μg/ml of the plasma membrane marker CM-Dil for 10 min. Note that GFP (green) and CM-Dil (red) are highly colocalized in tubular structures. Insets show higher magnification views of the areas indicated by boxes. Bar, 10 μm. (D–F) dRich physically interacts with dCIP4. (D) dRich interacts with the SH3 domain of dCIP4 via its proline-rich domain (PRD). In pull-down assays, lysates of HEK293 cells expressing an HA-tagged version of either full-length dRich (HA-dRich) or the C-terminal PRD of dRich (HA-dRich-PRD) were incubated with GST or GST fusion proteins of full-length dCIP4 (GST-dCIP4), a dCIP4 mutant deleting the SH3 domain (dCIP4ΔSH3), and the SH3 domain of dCIP4 (GST-dCIP4-SH3). Western blot analysis using anti-HA antibody was performed to detect pulled-down HA-dRich (top) and HA-dRich-PRD (bottom). Note that GST-dCIP4 and GST-dCIP4-SH3, but not GST-dCIP4ΔSH3 and GST alone, are able to efficiently pull down HA-dRich and that GST-dCIP4-SH3 precipitates HA-dRich-PRD at comparable levels with HA-dRich. (E) The fourth proline-rich motif of dRich mediates its interaction with dCIP4. In pull-down assays, GST-dCIP4-SH3 was incubated with total lysates of HEK293 cells transiently expressing HA-dRich, HA-dRichΔP4, HA-dRichΔP3-4, HA-dRichΔP2-4, or HA-dRichΔP1-4. Expression of the proteins in total lysates was confirmed by Western blotting using anti-HA antibody (bottom). Note that removal of the fourth proline-rich motif completely abolishes interaction between HA-dRich and GST-dCIP4-SH3. (F) dRich physically interacts with dCIP4 in cultured cells. Soluble extracts of S2R⁺ cells transiently expressing dRich-GFP were immunoprecipitated with IgG or anti-GFP antibody. The presence of endogenous dCIP4 in precipitates was determined by Western blot (WB) analysis using anti-dCIP4. Markers are given in kilodaltons.

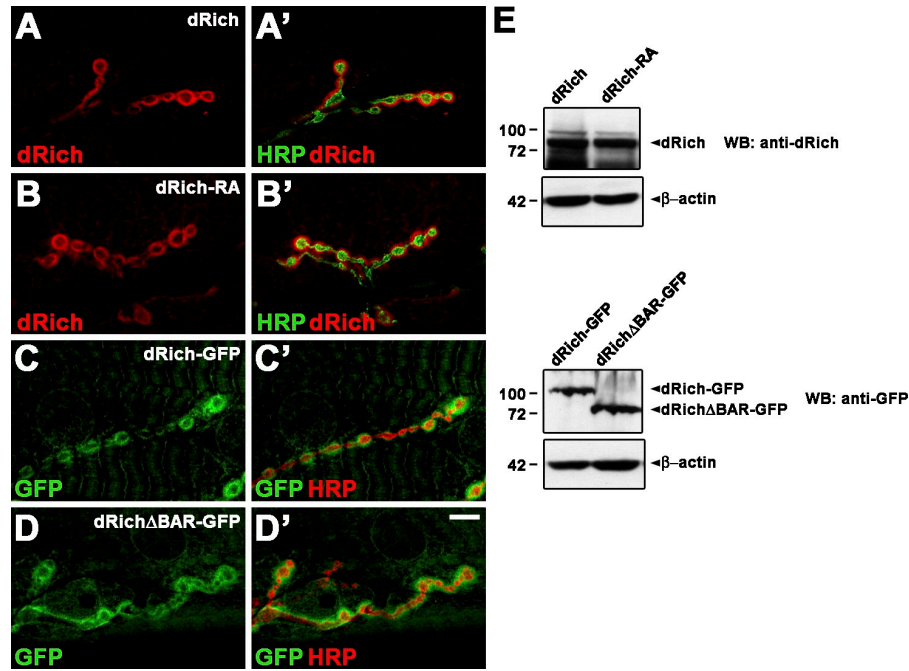


Figure S3. **Analysis of transgenic expression of dRich and its variants in *drich* mutants.** (A–D') Confocal images of third instar NMJ 6/7 in transgenic animals expressing dRich, dRich-R287A, dRich-GFP, or dRichΔBAR-GFP postsynaptically in the *drich*¹/*drich*² background. NMJs 6/7 doubly labeled with anti-HRP and anti-dRich (A and B) or anti-GFP (C and D) shown for *BG57-GAL4,drich*²/*UAS-drich,drich*¹ (dRich), *BG57-GAL4,drich*²/*UAS-drich-R287A,drich*¹ (dRich-RA), *BG57-GAL4,drich*²/*UAS-drich-GFP,drich*¹ (dRich-GFP), and *BG57-GAL4,drich*²/*UAS-drichΔBAR-GFP,drich*¹ (dRichΔBAR-GFP). (E) Western blots (WB) of muscle extracts from the genotypes shown in A–E probed with anti-dRich (top) or anti-GFP (bottom). β-Actin was used as a loading control. Markers are given in kilodaltons.

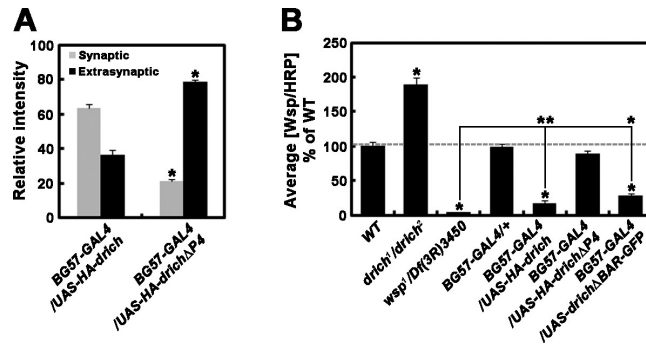


Figure S4. **Regulation of NMJ synaptic localization of both dRich and Wsp.** (A) Quantification of relative distribution of anti-HA immunoreactivity between the synaptic and extrasynaptic regions is shown for wild-type third instar larvae with postsynaptic expression of HA-dRich or HA-dRichΔP4. (B) Quantification of the ratio of mean Wsp to HRP staining intensities at NMJ 6/7 in the indicated genotypes. Values represent percentages of wild type (WT). All comparisons are with wild type unless indicated ($n > 15$). *, $P < 0.001$; **, $P < 0.01$. Error bars indicate mean ± SEM.

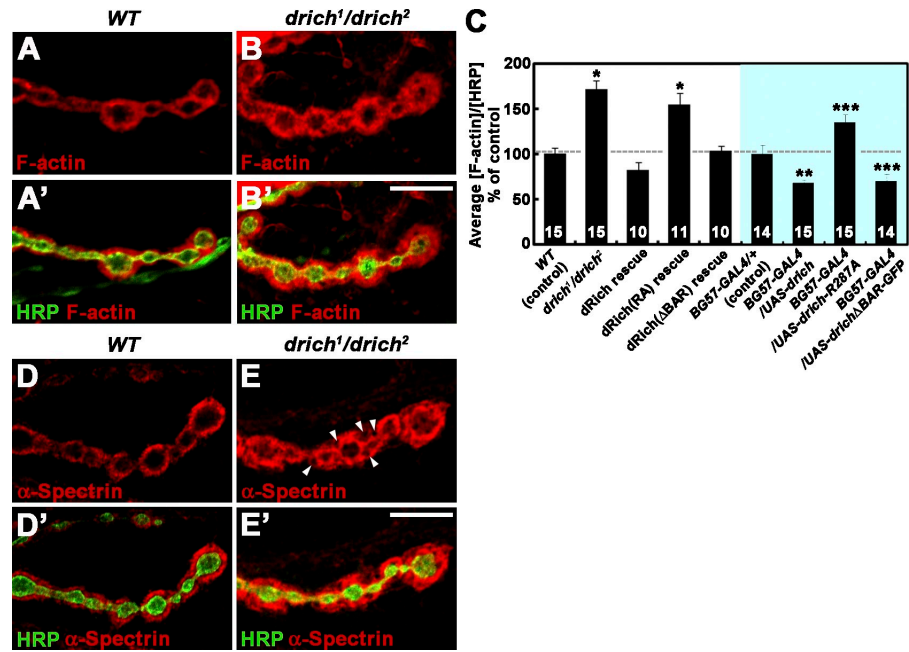


Figure S5. **dRich negatively regulates postsynaptic F-actin and α -spectrin.** (A–B') Confocal images of NMJ 12/13 branches in wild-type (A) and *drich¹/drich²* (B) mutant larvae doubly stained with rhodamine-conjugated phalloidin (red) and anti-HRP (green). Note that postsynaptic F-actin in *drich* is increased compared with wild-type larvae. (C) Quantification of the staining intensity of F-actin normalized to that of HRP. The genotypes analyzed include wild type (WT), *drich¹/drich²*, *BG57-GAL4,drich²/UAS-drich,drich¹* (dRich rescue), *BG57-GAL4,drich²/UAS-drich-R287A,drich¹* (dRich[RA] rescue), *BG57-GAL4,drich²/UAS-drichΔBAR-GFP,drich¹* (dRich[ΔBAR] rescue), *BG57-GAL4/+*, *BG57-GAL4/UAS-drich*, *BG57-GAL4/UAS-drich-R287A*, and *BG57-GAL4/UAS-drichΔBAR-GFP*. Values represent percentages of the corresponding control (wild type or *BG57-GAL4/+*). Statistically significant differences versus the corresponding control are indicated. *, $P < 0.001$; **, $P < 0.01$; ***, $P < 0.05$. Error bars indicate mean \pm SEM. (D–E') Confocal images of NMJ 6/7 double stained with anti-HRP (green) and anti- α -spectrin (red) antibodies in wild-type (D) and *drich¹/drich²* (E) larvae. The α -spectrin staining is missing in the several focal areas of the NMJ postsynapse in *drich* (arrowheads). Bars, 10 μ m.